Int J Adv Manuf Technol (2010) 49:281–292
DOI 10.1007/s00170-009-2390-3

ORIGINAL ARTICLE

A variable sampling interval EWMA chart for attributes

Eugenio K. Epprecht · Bruno F. T. Simões · Flávia C. T. Mendes

Received: 14 February 2009 / Accepted: 19 October 2009 / Published online: 18 November 2009

Abstract We propose a variable sampling interval exponentially weighted moving average (VSI *c* EWMA) chart for the average number of nonconformities in the sample, with the objective of improved detection of small to moderate increases in the process nonconformities rate. Using a Markov chain model for the calculations, we obtain optimal designs for this chart as well as for the fixed sampling interval *c* EWMA chart and compare the performances of the two control schemes in terms of their expected times to signal an out-of-control condition. The designs are optimal in the sense that they minimize the expected delay in the detection of upward shifts of a specified magnitude in the process nonconformities rate, while keeping the false alarm rate and the average sampling frequency at specified levels. The results reveal considerable gains in detection speed with the use of the VSI scheme. The optimal parameters found for each case are tabulated and may be used directly in practice. The results of the analysis, including the optimal design parameters tabulated, can also be extended to a VSI *np* EWMA chart for improved detection of small to moderate increases in the fraction nonconforming of the process provided that in-control fraction nonconforming is small.

Keywords Variable sampling interval · EWMA control chart · Attributes · Fraction nonconforming · Adaptive control charts · Statistical process control charts · Poisson EWMA · VSI

E. K. Epprecht (✉) · B. F. T. Simões · F. C. T. Mendes
PUC-Rio,
Rio de Janeiro, Brazil
e-mail: eke@puc-rio.br

1 Introduction

The widely used Shewhart's process control charts, whether for variables or for attributes, are slow in detecting small changes in the process parameters. The most classic alternatives for quicker detection of such disturbances are the use of supplementary run rules together with the detection criterion of "one point beyond the control limits", the cumulative sum (CUSUM) schemes, and the exponentially weighted moving average (EWMA) control charts. Other alternatives are control charts with double sampling and, since the pioneering work of Reynolds et al. [26], the control charts with variable parameters, or *adaptive control charts*. In the latter one, the values of one or more parameters of the charts (sample size, sampling interval, and control limit factor) are made variable as a function of the most recent information provided by the last point plotted. For example, see Reynolds et al. [26], Sawalapurkar et al. [31], Runger and Montgomery [29], Prabhu et al. [19, 20], and Costa [6–11].

Although the parameters of adaptive charts may be allowed to vary over a discrete set of values (see for instance Vaughan [34]) or even over a continuous interval (e.g., Capizzi and Masarotto [5]), most of the proposed schemes in the literature allow them to vary just between two values, for greater simplicity of the design and operation, and since several studies showed that the marginal benefit of using more than two values for such parameters was small and not worth the extra complexity [20, 21, 24, 28, 29, 35]. For the sampling interval in particular, Reynolds [21] has shown that using only two values is the optimal policy.

After having been applied to Shewhart charts, adaptive schemes have been applied to CUSUM and EWMA charts [1, 2, 5, 23, 25, 27, 30], resulting in control schemes still more sensitive to small and moderate shifts in the process parameters.

As pointed out by Tagaras [32], in a survey on adaptive control charts, most of the research on the subject has been devoted to control charts for variables. One decade after this survey, works on adaptive control charts for attributes still remain a minority. We can cite Vaughan [34], Epprecht and Costa [12], Luo and Wu [17], and Epprecht et al. [13].

In particular, if there are some works on adaptive EWMA charts for variables (as already mentioned) and if several (nonadaptive) EWMA charts for attributes have also been proposed [3, 14, 15, 33], to our knowledge, no investigation on adaptive schemes for EWMA charts for attributes has been reported in the literature.

In this paper, we propose a variable sampling interval EWMA (VSI c EWMA) chart for the average number of nonconformities in the sample, with the objective of improved detection of small to moderate increases in the process nonconformities rate. We obtain optimal designs for this chart as well as for the fixed sampling interval (FSI) c EWMA chart and compare the performances of the two control schemes in terms of their expected times to signal an out-of-control condition. The designs are optimal in the sense that they minimize the expected delay in the detection of upward shifts of a specified magnitude in the process nonconformities rate, while keeping the false alarm rate and the average sampling frequency at specified levels. The results reveal considerable gains in detection speed with the use of the VSI scheme. The optimal parameters found for each case are tabulated and may be used directly in practice.

The remainder of this paper is organized as follows: Sections 2 and 3 describe, respectively, the existing fixed sampling interval and the proposed variable sampling interval c EWMA charts; Section 4 presents the formal definition of the optimization problem and describes the solution method, while the details of the mathematical model are given in the "Appendix" at the end of the paper; the optimal designs found are then presented in Section 5, together with the performance comparison between the two schemes. Section 6 describes a VSI *np* EWMA chart and indicates how the results in this paper extend to it. The conclusions are in Section 7, which is followed by the references and by the "Appendix" mentioned.

2 The FSI c EWMA chart

Let c_t, t=1, 2,…, be the number of nonconformities observed in successive random samples (of constant size) from a production process. The sample can consist of a given number of discrete units, in the case of a discrete production process, or of any defined unit from a homogeneous output, for example, a square meter of fabric or 100 m of cable. Then, the EWMA statistic for the number of nonconformities is defined recursively by

$$Z_t = (1-\lambda)Z_{t-1} + \lambda c_t \tag{1}$$

where λ is a specified smoothing constant such that $0 < \lambda \leq 1$ and $Z_0 = c_0$, the in-control expected number of nonconformities in a sample.

More than one version of (fixed sampling interval) EWMA chart has been proposed in the literature for monitoring the number of nonconformities in the sample. Gan [15] proposed and analyzed three modified EWMA charts for monitoring the number of nonconformities: In one of them, called REWMA, Z_t is rounded to the nearest integer; in another one, the CEWMA chart, Z_t is increased to its ceiling (the smallest integer greater or equal to Z_t); and in the last of them, the FEWMA chart, Z_t is decreased to its floor (integer part). Borror et al. [3], in contrast, propose using the exact value of the Z_t statistic given in Eq. 1 in what they call a *Poisson EWMA control chart*, with a pair of control limits given by

$$\mathrm{UCL} = c_0 + A_{\mathrm{U}}\sqrt{\lambda c_0/(2-\lambda)} \tag{2}$$

$$\mathrm{LCL} = c_0 - A_{\mathrm{L}}\sqrt{\lambda c_0/(2-\lambda)} \tag{3}$$

where the term inside the square root is the asymptotic variance of Z_t. The control limit factors A_{U} and A_{L} may be chosen to be equal or different. The latter case is indicated by the authors cited as useful when the lower limit would otherwise be negative, preventing thereby the detection of downward shifts in the nonconformities rate.

They show that the out-of-control ARLs (expected number of samples until a true alarm) for their chart are in general smaller than those of Gan's REWMA, CEWMA, and FEWMA charts.

Alternatively, control limits based on the exact variance of c_t (which is equal to its asymptotic value multiplied by $\left[1-(1-\lambda)^{2t}\right]$) may be used instead of the constant asymptotic control limits in Eqs. 2 and 3. Montgomery [18] indicates the version with the exact limits; Borror et al. [3] just mention this alternative and focus on the constant limits version.

The FSI c EWMA chart with which we compare the performance of the VSI c EWMA chart is the *Poisson EWMA* chart by Borror et al. [3] since it have been shown to outperform Gan's [15] charts. We consider its one-sided version, without a lower control limit, to make a coherent comparison with the proposed VSI c EWMA chart, which is also one-sided, as will be seen next. We will denote its control limit factor by k rather than A_{U}. Like Borror et al. [3], we consider the constant UCL given in Eq. 2. Indeed, this is useful for the study of the chart's properties. If the exact limits were used instead, this would increase the sensitivity of the chart to special causes occurring before the beginning of the monitoring or soon after it, but the

steady-state performance of the chart would remain unchanged, and its performance measures would coincide with the values calculated assuming the constant limits. The false-alarm rate, however, would be slightly higher. This is true regarding the VSI chart as well.

3 The VSI *c* EWMA chart

The VSI *c* EWMA chart we propose corresponds to the one-sided Poisson EWMA chart (without a LCL) with the incorporation of a variable sampling interval procedure.

We focus on one-sided charts because we assume that the priority is to detect as quickly as possible small and moderate upward shifts in the process nonconformities rate, and one-sided charts will be more efficient against such shifts than their two-sided counterparts with the same ATS_0. As to downward shifts, we consider that their detection, while desirable, is not urgent and may be left to other procedures such as periodic off-line analyses of the c_t data.

For the VSI *c* EWMA chart, the recursive EWMA equation remains as in Eq. 1, as remains $Z_0=c_0$. The chart has one control limit, UCL, and a warning limit, WL, given by:

$$\mathrm{UCL} = c_0 + k\sqrt{\lambda c_0/(2-\lambda)} \tag{4}$$

$$\mathrm{WL} = c_0 + w\sqrt{\lambda c_0/(2-\lambda)} \tag{5}$$

where $w<k$. The chart is operated with two sampling intervals, a longer one, h_L, and a shorter one, h_S. The interval to be used at each time is determined by the position of the last EWMA value, according to the following rule: if $Z_t \leq$ WL, then the next sample is taken after a time h_L; if $WL < Z_t \leq UCL$, then the next sample is taken after a time h_S. This is illustrated in Fig. 1.

The basic idea is to wait less time to take the next sample when the process is more likely to be out of control, in order to reduce the delay in the detection of special causes, and to wait more time otherwise, in order to compensate for the reduced sampling intervals so as to maintain the average sampling frequency at a specified level.

The design parameters for the VSI *c* EWMA chart are therefore the smoothing constant λ, the control and warning limits factors k and w, and the long and short sampling intervals, h_L and h_S.

4 Optimization of the design: model and solution

4.1 Problem context and basic assumptions

The basic hypotheses we assume for the optimization of the designs and for comparison of the performances of the FSI and VSI *c* EWMA charts are the following: the number of nonconformities in the successive samples (of constant size) taken from the process is independent and identically distributed Poisson variables, with mean c; the process is in control, with $c=c_0$, when the monitoring starts; and the eventual occurrence of an assignable cause makes the mean increase abruptly to a higher level $c=c_1$, in which it stays until there is an intervention to bring it again to the in-control level c_0. This is the steady-state scenario (the process is initially in control and the assignable cause occurs at a random time)—as opposed to the zero-state scenario, in which the process is already out of control when the monitoring starts. We focus on the steady-state scenario considering that the zero-state scenario, when it occurs, constitutes just a transient situation. Should the process be out of control when the monitoring starts for the first time,

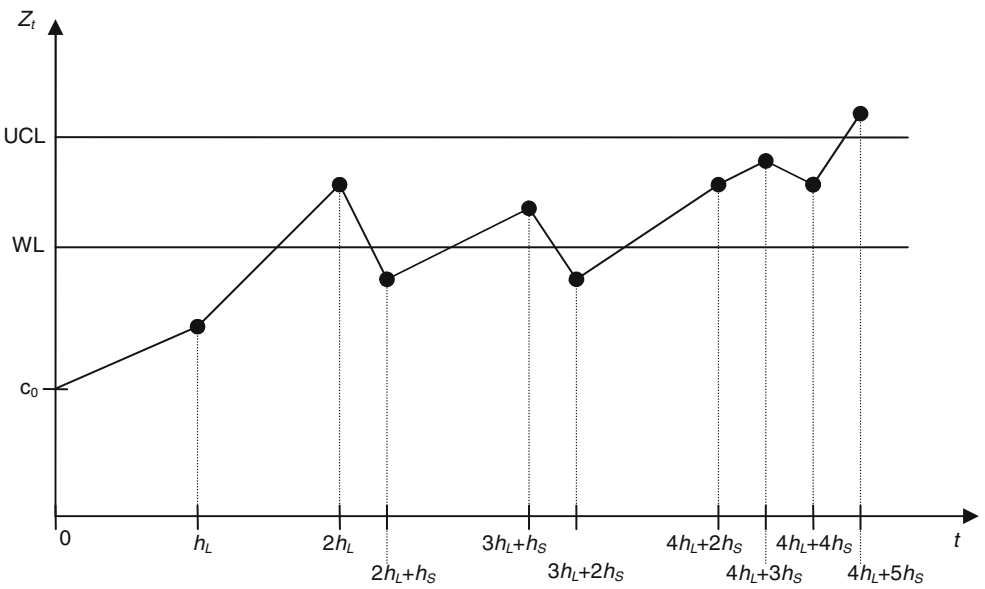

Fig. 1 The VSI *c* EWMA chart

then the eventual detection and removal of the assignable cause would put it in control for every restart.

4.2 Performance measures and problem specifications

The performance measure adopted in this work is the adjusted average time to signal (AATS), defined as the expected length of the time interval between the occurrence of the increase in the mean number of nonconformities and the signal given by the chart. This measure is used for comparing charts and also as the objective function to be minimized in the optimization of the charts designs.

The frequency of false alarms (in time) is measured by its inverse, the expected time until a false alarm, ATS_0. The minimum allowable value for ATS_0, $ATS_{0\ min}$, is a constraint for the optimization of the design and should be specified.

Other specification for the problem is the sampling frequency—which, too, in this study is specified by means of its inverse, h. For the FSI chart, h is simply the constant sampling interval. In the case of the VSI chart, the *average* sampling interval when the process is in control, $\overline{h}$, should be kept at the specified value h. Obviously, when the process goes out of control, the average sampling interval of the VSI chart is automatically reduced in order to reduce the time until the alarm, but the impact on the overall average sampling frequency should be small because the time until the true alarm should be much smaller than the mean time between special cause occurrences. This assumption has been adopted in many previous works on control charts with variable sampling intervals, whether explicitly stated (e.g., [7, 10]) or implicit in the requirement that the in-control average sampling interval should remain at a specified value [13]; these references are not exhaustive, just some examples.

In addition to h and $ATS_{0\ min}$, the specifications for the optimization of the design include the value of c_1 for which the AATS should be minimized, and the specifications for the VSI chart include the length of the shorter sampling interval, h_S. As it will be seen, the smaller the h_S, the smaller will be the AATS. For this reason, one should specify for h_S the minimum practicable value.

For convenience, we will refer henceforth to the factor of increase in c, $\gamma=c_1/c_0$, $\gamma>1$, rather than to c_1. According to this notation, the value of c_1 for which the AATS should be minimized can be indicated as $\gamma^* c_0$, and we will refer to γ^* instead of referring to, say, c_1^*.

From all above, the problem of optimization of the VSI c EWMA chart is, in formal notation,

$$\begin{aligned} &\text{Given } c_0, \gamma^*, h_S, \text{ and } h, \\ &\underset{\lambda,k,w,h_L}{\text{minimize}}\ AATS_{\gamma^*} \\ &\text{subject to} \\ &ATS_0 \geq ATS_{0\ min} \\ &\overline{h} = h \end{aligned} \qquad \text{(Expression 6)}$$

where $AATS_{\gamma^*}$ denotes the AATS for $c_1=\gamma^* c_0$. Since the smaller sampling interval, h_S, is specified, the decision variables are the smoothing constant λ, the factors k and w that correspond to the control limit and to the warning limit, and the longer sampling interval, h_L.

For the FSI c EWMA chart, the optimization problem is:

$$\begin{aligned} &\text{Given } c_0, \gamma^*, \text{ and } h, \\ &\underset{\lambda,k}{\text{minimize}}\ AATS_{\gamma^*} \\ &\text{subject to} \\ &ATS_0 \geq ATS_{0\ min} \end{aligned} \qquad \text{(Expression 7)}$$

For comparing the AATS performances of two or more charts designed for the same situation (that is, same c_0 and γ^*), they should have the same false-alarm rate and same average sampling frequency, that is, they should have been designed with the same specifications for $ATS_{0\ min}$ and h.

4.3 Solution method

For the VSI c EWMA chart, we developed a Markov chain model to calculate, as a function of c_0, c_1, λ, k, w, h_L, and h, the value of h_S that results in $\overline{h} = h$ and the resulting ATS_0 and AATS. This model was used by an optimization program to search for the optimal solution of the problem in Expression 6. The same model and program were used for the FSI c EWMA chart and Expression 7, just setting $h_L=h_S=\overline{h}$ and $w=k$.

The optimal designs were obtained through the Nelder–Mead simplex method of direct search, using the Matlab® function *fminsearch*. The constraint on the ATS_0 was implemented using a penalty function. The starting point for the search was obtained by a two-step procedure, using programs written in Microsoft Excel®: First, the range (0, 1) for λ was discretized and for each of the λ values considered, the value of k that gave the desired $ARL_0=ATS_0$ was determined and a search was conducted for the best value for w; in the next step, a grid search was conducted around the best solution thus obtained. During this search for the starting point for the Nelder–Mead algorithm as well as during the search for the optimal designs with the Nelder–Mead algorithm itself, the ATS_0 and $AATS_{\gamma^*}$ for each intermediate solution were calculated using the Markov chain model. Once the optimal designs were found, the model was also used to calculate their AATS profiles for the purposes of the performance analysis.

The model developed constitutes an extension of the one used by Borror et al. [3], which in its turn is a version for Poisson EWMA charts of the model by Lucas and Saccucci [16] for EWMA charts on the mean of a continuous variable. The basic principle is the same of the pioneering model by Brook and Evans [4] for CUSUM schemes,

namely, to discretize the interval between the control limits (in our case, the interval between 0 and the UCL) by dividing it into a number of subintervals, each one corresponding to a state of the chain. The number of subintervals should be sufficiently large to ensure good precision. Previous works (viz., [5]) have shown that a minimum of 40 to 50 subintervals is desirable and that 100 subintervals are enough for very precise results. We used 100 subintervals. Modifications were introduced to incorporate the variation of the sampling interval. Another difference from the model by Borror et al. [3] is that those authors considered the zero-state performance of their chart (measured by the out-of-control ARL—which, when multiplied by the sampling interval length h, yields the zero-state average time to signal) while we consider the steady-state performance of the charts (measured by the AATS). The model is described in detail in the "Appendix".

5 Results and performance comparison

Optimal designs were obtained for the FSI and VSI c EWMA charts, for all combinations of c_0=0.5, 1.0, 2.0, and 4.0 and γ^*=1.5 and 2.0 and with the constraints $ATS_0 \geq 200$ and $ATS_0 \geq 370$ time units. The time unit adopted to express the ATS_0 and all the other times (AATS, h, h_S, h_L) is the length of the (constant or average) sampling interval. In this unit, $\overline{h} = h = 1$. For the VSI charts, three values were considered for the smaller sampling interval h_S, namely 0.50, 0.25, and 0.10.

Table 1 presents the results for $ATS_0 \geq 200$ and Table 2 presents the results for $ATS_0 \geq 370$. These tables also give, for each design, the exact ATS_0 as well as the AATS not only for γ^* but also for a number of values of γ between 1.5 and 4.0. For easier visualization, Tables 3 and 4 give, for each VSI chart in Tables 1 and 2 respectively, the percent reduction in the AATSs with respect to the FSI chart, and Fig. 2 shows the AATS curves of the FSI and three corresponding VSI charts (with h_S=0.50, 0.25, and 0.10) for the case c_0=2.0 and γ^*=1.5, with $ATS_{0\ min}$=370. The sets of curves for the remaining cases in Tables 1 and 2 have a similar aspect. For this reason, as well as for space limitation and finally because such curves just display information already contained in the tables, only the case in Fig. 2 is displayed, as an example.

From these tables and figures, it is easy to see that:

- In the range of values of c_0 considered, the VSI scheme can provide considerable reductions in the AATS of the c EWMA chart not only for the specific value of γ for which the design was optimized, γ^*, but also for all values of γ between 1.5 and 4.0 at least. The only and very few exceptions are the cases where c_0, γ, and γ^* take the largest values in their respective ranges together, i.e., c_0=4.0, γ=4.0, and γ^*=2.0. In these cases, the VSI chart's AATSs are larger than those of the FSI chart (and result in negative values in Tables 3 and 4). Nevertheless, these VSI designs with larger AATS for γ=4.0 still give smaller AATS than the FSI chart for smaller values of γ. In particular, for γ=2.0 (which is the value γ^* for which they were optimized), the reduction they provide in the AATS varies from 26.7% to 53.3%, depending on h_S and on ATS_0.
- Depending on the case, the reduction in the AATS with the VSI scheme may attain 56.7%. The reductions are greater with $ATS_{0\ min}$=370 than with $ATS_{0\ min}$=200. They also tend to be more significant for larger values of c_0, at least until c_0=2. For c_0=4, these gains in detection speed are sometimes lower than for c_0=2 (including the extreme cases mentioned in which the FSI chart outperforms the VSI scheme).
- The percent AATS reduction with the VSI scheme for values of $\gamma \geq \gamma^*$ is larger for smaller values of γ. In other words, the smaller the increase in the mean number of nonconformities, the greater will be the advantage in the use of the VSI scheme.
- The smaller the value of h_S, all else constant, the smaller are the AATS values—a result that coincides with the findings of Reynolds [21, 22], Reynolds and Arnold [24], Reynolds et al. [27], Runger and Montgomery [29], Prabhu et al. [20], Costa [10], Epprecht et al. [13], among others. The reductions in the AATS, however, are not proportional to the reductions in h_S (again a result consistent with previous works, for instance [13]): As h_S decreases, the marginal gain also decreases. This can be easily appreciated in Fig. 2. Working with $h_S = 0.25\overline{h}$ is already very effective. This result is important and convenient because too short sampling intervals may not be feasible in several practical situations.

6 A VSI *np* EWMA chart

For controlling a process by the number of defective units in the sample, a VSI *np* EWMA chart can be defined and operated in the same way as the VSI c EWMA chart, having as parameters the smoothing constant λ, the control and warning limits factors k and w, and the large and short sampling intervals, h_L and h_S. There will be only two differences: In the recursive equation of the EWMA, the number of defective units in the t-th sample, d_t, would be used instead of the number of nonconformities, so the equation becomes

$$Z_t = (1-\lambda)Z_{t-1} + \lambda d_t \tag{6}$$

Table 1 Optimal designs and AATS profiles for $ATS_{0\ min}$=200

c_0	γ*	Optimal designs	ATS_0	AATS values					
		FSI (λ, k, h)		γ					
		VSI (λ, w, k, h_S, h_L)		1.5	2	2.5	3	3.5	4
0.5	1.5	FSI (0.0948, 2.3658, 1.00)	200.23	27.74	12.03	7.43	5.33	4.15	3.39
		VSI (0.1005, 0.0600, 2.3751, 0.50, 1.3244)	200.02	22.69	9.33	5.74	4.14	3.24	2.67
		VSI (0.0647, 0.0650, 2.1069, 0.25, 1.4421)	200.16	20.04	8.58	5.44	3.99	3.16	2.63
		VSI (0.1188, 0.0810, 2.4760, 0.10, 1.5933)	200.00	19.08	7.19	4.38	3.19	2.53	2.12
	2.0	FSI (0.0961, 2.3660, 1.00)	200.06	27.82	12.02	7.41	5.31	4.13	3.37
		VSI (0.1135, 0.0930, 2.4500, 0.50, 1.3265)	200.40	23.11	9.30	5.65	4.05	3.16	2.60
		VSI (0.1095, 0.0920, 2.4240, 0.25, 1.4502)	200.22	20.55	8.03	4.90	3.54	2.79	2.31
		VSI (0.1188, 0.0810, 2.4760, 0.10, 1.5933)	200.00	19.08	7.19	4.38	3.19	2.53	2.12
1.0	1.5	FSI (0.1092, 2.3428, 1.00)	200.05	18.01	7.54	4.64	3.33	2.59	2.11
		VSI (0.1055, 0.0312, 2.3316, 0.50, 1.3623)	200.41	13.93	5.80	3.64	2.66	2.10	1.75
		VSI (0.1192, 0.2935, 2.4033, 0.25, 1.3522)	200.02	12.51	4.91	3.05	2.23	1.77	1.48
		VSI (0.0947, 0.1979, 2.2531, 0.10, 1.4864)	200.26	11.27	4.68	2.99	2.22	1.78	1.50
	2.0	FSI (0.1109, 2.3470, 1.00)	200.18	18.06	7.53	4.63	3.32	2.58	2.10
		VSI (0.1114, 0.1780, 2.3290, 0.50, 1.2922)	200.28	14.12	5.78	3.60	2.61	2.06	1.71
		VSI (0.1192, 0.2935, 2.4033, 0.25, 1.3522)	200.02	12.51	4.91	3.05	2.23	1.77	1.48
		VSI (0.2040, 0.0466, 2.6837, 0.10, 1.6318)	200.04	11.72	4.03	2.46	1.83	1.48	1.27
2.0	1.5	FSI (0.1044, 2.2656, 1.00)	200.14	11.25	4.80	3.00	2.18	1.70	1.40
		VSI (0.1045, 0.0979, 2.2731, 0.50, 1.3310)	200.59	8.61	3.74	2.40	1.77	1.42	1.20
		VSI (0.1529, 0.1307, 2.4285, 0.25, 1.5120)	200.05	7.14	2.96	1.91	1.45	1.19	1.03
		VSI (0.2152, 0.0723, 2.6164, 0.10, 1.6669)	200.21	6.29	2.45	1.61	1.26	1.08	0.97
	2.0	FSI (0.2198, 2.6200, 1.00)	200.10	12.11	4.48	2.63	1.84	1.41	1.14
		VSI (0.2201, 0.1210, 2.6210, 0.50, 1.3189)	200.15	8.87	3.29	2.01	1.46	1.17	0.99
		VSI (0.3256, 0.0545, 2.7927, 0.25, 1.5338)	200.14	8.02	2.63	1.61	1.22	1.02	0.90
		VSI (0.3498, 0.1140, 2.8140, 0.10, 1.5691)	200.80	7.35	2.26	1.41	1.10	0.95	0.87
4.0	1.5	FSI (0.1092, 2.2424, 1.00)	200.13	7.07	3.07	1.94	1.41	1.10	0.90
		VSI (0.2090, 0.1726, 2.5258, 0.50, 1.3180)	200.56	5.08	2.08	1.33	1.01	0.83	0.73
		VSI (0.2903, 0.0298, 2.6646, 0.25, 1.6144)	200.03	4.11	1.69	1.15	0.95	0.85	0.79
		VSI (0.3050, 0.0332, 2.6682, 0.10, 1.6823)	200.32	3.51	1.48	1.07	0.92	0.86	0.83
	2.0	FSI (0.3314, 2.710, 1.00)	200.17	7.54	2.59	1.49	1.03	0.79	0.65
		VSI (0.3600, 0.1180, 2.7410, 0.50, 1.3420)	200.00	5.40	1.90	1.18	0.89	0.75	0.67
		VSI (0.4929, 0.3233, 2.8426, 0.25, 1.3626)	200.03	5.07	1.53	0.97	0.79	0.71	0.67
		VSI (0.4930, 0.3320, 2.8433, 0.10, 1.4351)	200.04	4.34	1.33	0.91	0.78	0.73	0.71

with $Z_0=np_0$, where n is the sample size and p_0 is the in-control fraction defective of the process. The other difference is the expressions for the control and warning limits that will be

$$\mathrm{UCL} = np_0 + k\sqrt{\lambda np_0(1-p_0)/(2-\lambda)} \tag{7}$$

$$\mathrm{WL} = np_0 + w\sqrt{\lambda np_0(1-p_0)/(2-\lambda)} \tag{8}$$

The Markov chain model used for the VSI c EWMA chart can also be used to compute the performance measures of the VSI np EWMA chart just substituting the binomial distribution for the Poisson in the computation of the transition probabilities.

However, given the Poisson approximation to the binomial distribution, expressions 7 and 8 would yield limits very close the ones given by Eqs. 4 and 5 with $c_0=np_0$ when p_0 is small and n is large. If, in addition, $p_1=\gamma p_0$ is also small, then the transition probabilities are also well approximated by the Poisson distribution. As a conse-

Table 2 Optimal designs and AATS profiles for $ATS_{0\ min}=370$

c_0	γ^*	Optimal designs	ATS_0	AATS values					
		FSI (λ, k, h)		γ					
		VSI (λ, w, k, h_S, h_L)		1.5	2	2.5	3	3.5	4
0.5	1.5	FSI (0.0918, 2.6851, 1.00)	370.40	37.49	14.79	8.82	6.22	4.79	3.89
		VSI (0.1061, 0.0916, 2.7607, 0.50, 1.3363)	370.23	29.79	10.92	6.46	4.58	3.55	2.90
		VSI (0.0578, 0.2139, 2.4405, 0.25, 1.4124)	370.88	24.11	9.74	6.10	4.45	3.52	2.91
		VSI (0.0588, 0.2029, 2.4382, 0.10, 1.4847)	371.03	22.07	8.78	5.51	4.04	3.20	2.66
	2.0	FSI (0.0918, 2.6851, 1.00)	370.40	37.49	14.79	8.82	6.22	4.79	3.89
		VSI (0.1061, 0.0916, 2.7607, 0.50, 1.3363)	370.23	29.79	10.92	6.46	4.58	3.55	2.90
		VSI (0.1172, 0.0968, 2.8142, 0.25, 1.4914)	370.32	26.21	8.99	5.28	3.76	2.93	2.41
		VSI (0.1208, 0.0784, 2.8389, 0.10, 1.6513)	370.49	23.44	7.78	4.61	3.33	2.63	2.19
1.0	1.5	FSI (0.0630, 2.4198, 1.00)	370.17	22.13	9.36	5.85	4.25	3.33	2.73
		VSI (0.1056, 0.0504, 2.6954, 0.50, 1.3872)	370.02	16.93	6.60	4.06	2.94	2.32	1.92
		VSI (0.0646, 0.0409, 2.4271, 0.25, 1.5639)	370.33	14.18	6.12	3.93	2.91	2.33	1.95
		VSI (0.0644, 0.0325, 2.4159, 0.10, 1.6767)	370.34	12.70	5.53	3.59	2.68	2.16	1.82
	2.0	FSI (0.1126, 2.7293, 1.00)	370.28	23.40	8.94	5.34	3.79	2.93	2.38
		VSI (0.1130, 0.1888, 2.7266, 0.50, 1.3081)	370.58	17.29	6.53	3.98	2.87	2.25	1.86
		VSI (0.1147, 0.2701, 2.7375, 0.25, 1.3789)	370.26	14.66	5.39	3.31	2.40	1.90	1.59
		VSI (0.1863, 0.0469, 2.9705, 0.10, 1.7151)	370.08	13.56	4.34	2.65	1.96	1.60	1.37
2.0	1.5	FSI (0.0636, 2.3788, 1.00)	370.10	13.89	6.03	3.82	2.79	2.19	1.80
		VSI (0.1001, 0.0922, 2.5855, 0.50, 1.3422)	370.88	10.02	4.20	2.66	1.96	1.57	1.31
		VSI (0.1842, 0.0860, 2.8772, 0.25, 1.5697)	370.32	8.17	3.08	1.95	1.47	1.21	1.06
		VSI (0.1966, 0.0951, 2.8951, 0.10, 1.6718)	370.30	6.96	2.61	1.71	1.32	1.12	1.00
	2.0	FSI (0.2238, 2.9548, 1.00)	370.40	15.72	5.27	3.00	2.07	1.57	1.27
		VSI (0.2275, 0.1171, 2.9546, 0.50, 1.3519)	370.37	10.95	3.70	2.20	1.58	1.26	1.06
		VSI (0.2320, 0.1275, 2.9617, 0.25, 1.5139)	370.51	8.68	2.94	1.82	1.36	1.12	0.98
		VSI (0.3420, 0.1113, 3.1276, 0.10, 1.6311)	370.01	8.69	2.40	1.49	1.16	1.00	0.91
4.0	1.5	FSI (0.1143, 2.5971, 1.00)	370.51	8.33	3.46	2.16	1.57	1.22	1.00
		VSI (0.2056, 0.1836, 2.8249, 0.50, 1.3195)	370.10	5.88	2.28	1.44	1.08	0.89	0.77
		VSI (0.2990, 0.0900, 2.9663, 0.25, 1.5645)	370.08	4.70	1.76	1.18	0.96	0.85	0.79
		VSI (0.2768, 0.0700, 2.9382, 0.10, 1.7309)	370.06	3.80	1.60	1.14	0.98	0.90	0.87
	2.0	FSI (0.3402, 3.0039, 1.00)	370.25	9.65	2.99	1.66	1.13	0.85	0.69
		VSI (0.3856, 0.1200, 3.0342, 0.50, 1.3231)	370.42	6.86	2.11	1.26	0.93	0.77	0.68
		VSI (0.4664, 0.3000, 3.1081, 0.25, 1.3808)	370.36	5.97	1.66	1.04	0.83	0.73	0.69
		VSI (0.4499, 0.3238, 3.1063, 0.10, 1.4389)	371.36	4.88	1.40	0.94	0.80	0.74	0.72

quence, in these cases, the performances of the corresponding *np* and *c* charts (when $np_0=c_0$) would be practically identical, and the results of the analysis done for VSI *c* EWMA charts can be directly applied to VSI *np* EWMA charts. In particular, the optimal design parameters (λ, k, w, h_L, and h_S) obtained for the VSI *c* EWMA chart may be used without change for the corresponding VSI *np* EWMA chart, and the ATS_0 and AATSs of the VSI *np* EWMA chart would be very close to the values of the corresponding VSI *c* EWMA chart in Tables 1 and 2.

7 Conclusions

The proposed VSI *c* EWMA chart is more efficient than the fixed parameter *c* EWMA chart at detecting increases in the process nonconformities rate. For processes with c_0 ranging from 0.5 to 4.0, when the charts are optimized for upward shifts of 50% to 100% in *c*, and for ATS_0 equal to 200 or 370 times the average sampling interval, the reductions in the AATS of the *c* EWMA chart obtained with the incorporation of the VSI procedure may attain 50% or even a little more, depending on the case and on the shift.

Table 3 Percent reductions in the AATS with respect to the FSI chart for $ATS_{0\ min}=200$

c_0	γ^*	Design	ATS_0	AATS reduction (%)					
		FSI (λ, k, h)		γ					
		VSI (λ, w, k, h_S, h_L)		1.5	2	2.5	3	3.5	4
0.5	1.5	FSI (0.0948, 2.3658, 1.00)	200.07						
		VSI (0.1005, 0.0600, 2.3751, 0.50, 1.3244)	200.02	18.2	22.5	22.8	22.4	21.9	21.4
		VSI (0.0647, 0.0650, 2.1069, 0.25, 1.4421)	200.16	27.8	28.6	26.8	25.2	23.8	22.6
		VSI (0.1188, 0.0810, 2.4760, 0.10, 1.5933)	200.15	31.2	40.2	41.0	40.2	39.0	37.6
	2.0	FSI (0.0961, 2.3660, 1.00)	200.06						
		VSI (0.1135, 0.0930, 2.4500, 0.50, 1.3265)	200.40	16.9	22.7	23.7	23.7	23.4	23.0
		VSI (0.1095, 0.0920, 2.4240, 0.25, 1.4502)	200.22	26.2	33.2	33.9	33.4	32.6	31.6
		VSI (0.1188, 0.0810, 2.4760, 0.10, 1.5933)	200.00	31.4	40.2	40.8	39.9	38.7	37.3
1.0	1.5	FSI (0.1092, 2.3428, 1.00)	200.05						
		VSI (0.1055, 0.0312, 2.3316, 0.50, 1.3623)	200.41	22.6	23.0	21.6	20.2	18.8	17.3
		VSI (0.1192, 0.2935, 2.4033, 0.25, 1.3522)	200.40	30.5	34.8	34.2	33.0	31.5	29.8
		VSI (0.0947, 0.1979, 2.2531, 0.10, 1.4864)	200.40	37.4	37.9	35.5	33.3	31.1	28.8
	2.0	FSI (0.1109, 2.3470, 1.00)	200.18						
		VSI (0.1114, 0.1780, 2.3290, 0.50, 1.2922)	200.28	21.8	23.3	22.3	21.2	20.1	18.9
		VSI (0.1192, 0.2935, 2.4033, 0.25, 1.3522)	200.34	30.7	34.8	34.0	32.7	31.2	29.5
		VSI (0.2040, 0.0466, 2.6837, 0.10, 1.6318)	200.26	35.1	46.4	46.7	44.9	42.4	39.4
2.0	1.5	FSI (0.1044, 2.2656, 1.00)	200.14						
		VSI (0.1045, 0.0979, 2.2731, 0.50, 1.3310)	200.59	23.4	22.0	20.2	18.5	16.5	14.3
		VSI (0.1529, 0.1307, 2.4285, 0.25, 1.5120)	200.04	36.6	38.3	36.3	33.5	30.2	26.1
		VSI (0.2152, 0.0723, 2.6164, 0.10, 1.6669)	200.21	44.1	48.9	46.2	42.0	36.8	30.5
	2.0	FSI (0.2198, 2.6200, 1.00)	200.10						
		VSI (0.2201, 0.1210, 2.6210, 0.50, 1.3189)	200.15	26.8	26.5	23.7	20.6	17.1	13.3
		VSI (0.3256, 0.0545, 2.7927, 0.25, 1.5338)	200.01	33.7	41.3	38.8	33.9	27.8	20.6
		VSI (0.3498, 0.1140, 2.8140, 0.10, 1.5691)	200.80	39.3	49.6	46.5	40.4	32.6	23.5
4.0	1.5	FSI (0.1092, 2.2424, 1.00)	200.13						
		VSI (0.2090, 0.1726, 2.5258, 0.50, 1.3180)	200.56	28.2	32.5	31.4	28.5	24.4	19.4
		VSI (0.2903, 0.0298, 2.6646, 0.25, 1.6144)	200.07	41.9	45.1	40.4	32.8	23.2	12.2
		VSI (0.3050, 0.0332, 2.6682, 0.10, 1.6823)	200.32	50.4	51.9	44.8	34.4	21.8	7.6
	2.0	FSI (0.3314, 2.710, 1.00)	200.17						
		VSI (0.3600, 0.1180, 2.7410, 0.50, 1.3420)	200.00	28.5	26.7	20.8	13.3	4.9	-3.2
		VSI (0.4929, 0.3233, 2.8426, 0.25, 1.3626)	200.75	32.7	41.0	34.6	23.7	10.3	-3.2
		VSI (0.4930, 0.3320, 2.8433, 0.10, 1.4351)	201.41	42.5	48.8	39.1	24.3	7.0	-9.9

The reductions are greater for smaller values of the shorter sampling interval, a result which is consistent with the behavior of other VSI charts in the literature. The advantages of the VSI over the fixed-parameter c EWMA chart dissipate only for the extreme values considered of both c_0 and c_1, namely for $c_0=4$ and increases of 300% in the average nonconformities rate c and only regarding the design optimized for detecting increases of 100% in c. The designs that are optimal for detecting increases of 50% in c still give AATSs for these extreme values of c_0 and c_1 that are between 7.6% and 22.7% smaller than the ones of the FSI c EWMA chart.

In process control by the number of nonconformities (as in process control by attributes in general), there may be operational obstacles to the variation of the sample size, which, in the case of high quality processes, may need to be large so as to allow a minimum count of nonconformities to occur. In such cases, the implementation of variable sample size procedures may be unfeasible because they may either require too small a smaller sample size for a minimum

Table 4 Percent reductions in the AATS with respect to the FSI chart for $ATS_{0\ min}=370$

c_0	γ^*	Design	ATS_0	AATS reduction (%)					
		FSI (λ, k, h)		γ					
		VSI (λ, w, k, h_S, h_L)		1.5	2	2.5	3	3.5	4
0.5	1.5	FSI (0.0918, 2.6851, 1.00)	370.40						
		VSI (0.10534, 0.3198, 2.7577, 0.50, 1.2244)	370.07	20.6	10.3	26.7	26.4	26.0	25.5
		VSI (0.0578, 0.2139, 2.4405, 0.25, 1.4124)	370.88	35.7	13.5	30.9	28.5	26.6	25.2
		VSI (0.0588, 0.2029, 2.4382, 0.10, 1.4847)	371.03	41.1	16.0	37.5	35.1	33.2	31.6
	2.0	FSI (0.1061, 2.7604, 1.00)	370.23						
		VSI (0.1061, 0.0916, 2.7607, 0.50, 1.3363)	370.23	20.6	26.1	26.7	26.4	26.0	25.5
		VSI (0.1172, 0.0968, 2.8142, 0.25, 1.4914)	370.32	30.1	39.2	40.2	39.7	38.9	38.0
		VSI (0.1208, 0.0784, 2.8389, 0.10, 1.6513)	370.49	37.5	47.4	47.7	46.5	45.1	43.6
1.0	1.5	FSI (0.0630, 2.4198, 1.00)	370.17						
		VSI (0.1056, 0.0504, 2.6954, 0.50, 1.3872)	370.02	23.5	29.5	30.6	30.6	30.3	29.8
		VSI (0.0646, 0.0409, 2.4271, 0.25, 1.5639)	370.33	36.0	34.6	32.8	31.4	30.0	28.6
		VSI (0.0644, 0.0325, 2.4159, 0.10, 1.6767)	370.34	42.6	40.9	38.7	36.9	35.2	33.4
	2.0	FSI (0.1126, 2.7293, 1.00)	370.28						
		VSI (0.1130, 0.1888, 2.7266, 0.50, 1.3081)	370.58	26.1	26.9	25.5	24.2	23.0	21.8
		VSI (0.1147, 0.2701, 2.7375, 0.25, 1.3789)	370.26	37.4	39.7	38.1	36.5	34.9	33.3
		VSI (0.1863, 0.0040, 2.9705, 0.10, 1.7151)	370.08	42.0	51.4	50.4	48.1	45.4	42.4
2.0	1.5	FSI (0.0636, 2.3788, 1.00)	370.10						
		VSI (0.1001, 0.0922, 2.5855, 0.50, 1.3422)	370.88	27.8	30.5	30.4	29.6	28.5	27.1
		VSI (0.1842, 0.0860, 2.8772, 0.25, 1.5697)	370.32	41.1	49.0	48.9	47.3	44.7	41.4
		VSI (0.1966, 0.0951, 2.8951, 0.10, 1.6718)	370.30	49.9	56.7	55.4	52.6	48.9	44.3
	2.0	FSI (0.2238, 2.9548, 1.00)	370.40						
		VSI (0.2275, 0.1171, 2.9546, 0.50, 1.3519)	370.37	30.4	29.8	26.7	23.6	20.2	16.5
		VSI (0.2320, 0.1275, 2.9617, 0.25, 1.5139)	370.51	44.8	44.1	39.3	34.3	28.7	22.3
		VSI (0.3420, 0.1113, 3.1276, 0.10, 1.6311)	370.01	44.7	54.4	50.5	44.2	36.6	27.9
4.0	1.5	FSI (0.1143, 2.5971, 1.00)	370.51						
		VSI (0.2056, 0.1836, 2.8249, 0.50, 1.3195)	370.10	29.4	34.0	33.3	30.7	27.1	22.7
		VSI (0.2990, 0.0900, 2.9663, 0.25, 1.5645)	370.08	43.5	49.0	45.4	38.9	30.7	21.2
		VSI (0.2768, 0.0700, 2.9382, 0.10, 1.7309)	370.06	54.4	53.8	47.1	37.7	26.2	13.1
	2.0	FSI (0.3402, 3.0039, 1.00)	370.25						
		VSI (0.3856, 0.1200, 3.0342, 0.50, 1.3231)	370.42	28.9	29.5	24.5	17.6	9.4	1.0
		VSI (0.4664, 0.3000, 3.1081, 0.25, 1.3808)	370.36	38.1	44.5	37.7	26.9	13.8	0.0
		VSI (0.4498, 0.3218, 3.1067, 0.10, 1.4389)	371.40	49.4	53.3	43.3	29.3	12.6	-4.7

count of nonconformities to be observed or too large a larger sample size to be practicable, or both. Moreover, the increase in the power of the test which is the purpose of the increase in the sample size is damped down by the smoothing in the case of EWMA charts. Since the EWMA is a weighted average of the samples statistics, a *sequence* of large samples would be required for the effect of the larger sample size to become influent. The variation of the sampling interval, in contrast, has a direct and immediate impact on the *time* until the signal. In short, with EWMA charts, the variation of the sampling interval should be much more effective than the variation of the sample size—an expectation corroborated by the results in Reynolds and Arnold [25]. The proposed VSI c EWMA chart becomes then an excellent option for monitoring the nonconformities rate of a process.

Tables 1 and 2 provide guidance for the user on the choice of parameters for the design of VSI c EWMA charts with ATS_0 of 200 or 370. If one of the values of c_0 in these tables coincides with the in-control number of nonconformities in the sample or can be adopted as the acceptable quality level or still if the sample size can be used that

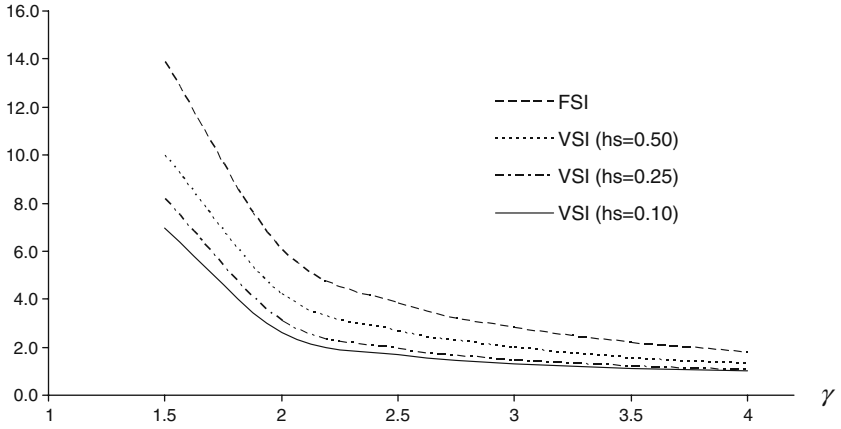

Fig. 2 AATS profiles of the optimal designs for $ATS_{0\ min}$= 370, c_0=2.0 and γ^*=1.5

makes c_0 coincide with one of the values in the tables, then one of the designs given in these tables may be adopted directly.

These tables can also be useful for designing VSI *np* EWMA charts when p_0 is small and the sample size n is such that np_0 coincides with one of the c_0 values in the tables, in the way indicated in Section 6.

Acknowledgments This work was partly supported by the Brazilian funding agencies Conselho Nacional de Desenvolvimento Científico e Tecnológico and Coordenação de Aperfeiçoamento de Pessoal de Nível Superior. This paper has been finished when the first author was in a sabbatical year at the Departamento de Estadística y Investigación Operativa Aplicadas y Calidad of the Universidad Politécnica de Valencia, Spain.

Appendix: Markov chain model of the VSI *c* EWMA

Let the interval (0, UCL] be divided into M subintervals of the same width L:

$$L = \mathrm{UCL}/M \tag{9}$$

For modeling purposes, it is convenient that WL be in the frontier between two subintervals. This can be achieved by forcing it to be an integer multiple of L. This will not constrain the flexibility of the design if M is large so that L is small. Formally, WL=$A\times L$, where A is an integer between 0 and M. So, there are A subintervals below WL and B=$M-A$ subintervals between WL and UCL.

The lower bound, midpoint, and upper bound of the i-th subinterval are given, respectively, by

$$l_j = (j-1)L \tag{10}$$

$$m_j = (j-0.5)L \tag{11}$$

$$u_j = jL \tag{12}$$

The index, i_0, of the subinterval that contains the value c_0 is

$$i_0 = \lceil c_0/L \rceil \tag{13}$$

where $\lceil x \rceil$ denotes the smallest integer greater or equal to x.

A Markov chain can be defined whose state in time t corresponds to the subinterval that contains Z_t. States 1 to A correspond to the subintervals below WL, and states A +1 to M correspond to the subintervals between WL and UCL. State M +1 is absorbing and corresponds to Z_t>UCL.

To compute the probability q_{ij} of the transition from a transient state i to another transient state j in one step, let us assume that when Z_t belongs to a given subinterval, its value coincides with the midpoint of that subinterval. The larger the number of subintervals M, the better is the quality of the approximation. It has been verified empirically [5] that M>50 yields good, that is, stable, results; most authors use about 100 subintervals. We used M=100.

Considering the EWMA recursive Eq. 1, the probability of transition from state i in time t-1 to state j in time t is then given by:

$$q_{ij} = \mathrm{P}\left[l_j < \lambda c_t + (1-\lambda)Z_{t-1} \le u_j | Z_{t-1} = m_i\right] \tag{14}$$

After substituting expressions 10 to 12 in Eq. 14, simple algebraic manipulations lead to

$$q_{ij} = P[a < c_t \le b] \tag{15}$$

where

$$a = \frac{L}{2\lambda}[2(j-1) - (1-\lambda)(2i-1)] \tag{16}$$

$$b = \frac{L}{2\lambda}[2j - (1-\lambda)(2i-1)] \tag{17}$$

and where the probability in Eq. 15 is calculated according to the Poisson distribution for c_t, with mean equal to γc_0. The probabilities q_{ij} obtained with γ=1 are the elements of the matrix $\mathbf{Q}_0$, the *in-control* matrix of transition probabil-

ities between transient states; with $\gamma>1$, they are the elements of $\mathbf{Q}_1$, the *out-of-control* transition probabilities matrix.

In either case, the element n_{ij} of the matrix

$$\mathbf{N} = (\mathbf{I} - \mathbf{Q})^{-1} \tag{18}$$

corresponds to the conditional expected number of visits to transient state j given that the initial state is state i. Again, there are two cases: with $\mathbf{Q}=\mathbf{Q}_0$, Eq. 18 gives the matrix $\mathbf{N}_0$, whose elements are the expected numbers of visits to transient states in the in-control phase, while with $\mathbf{Q}=\mathbf{Q}_1$, this equation gives the matrix $\mathbf{N}_1$, whose elements are the expected numbers of visits to transient states in the out-of-control phase.

Denote by $\mathbf{v}$ the $M\times 1$ vector of initial state probabilities for the in-control phase. Since $Z_0=c_0$, this vector has all elements equal to zero with the exception of the i_0-th element, which is equal to 1. Then, the expected numbers of visits to each transient state in the in-control phase are the elements of the vector $\mathbf{n}$, given by

$$\mathbf{n'} = \mathbf{v'N_0} \tag{19}$$

Note that $\mathbf{n}'$ is the i_0-th row of $\mathbf{N}_0$.

The ARL_0 is then given by:

$$\mathrm{ARL}_0 = \mathbf{n'1} \tag{20}$$

where $\mathbf{1}$ is a column vector of ones of dimension M.

The vector $\mathbf{r}$ (of dimension M) that gives the expected relative frequency of visits to each transient state during the in-control phase is given by

$$\mathbf{r} = (1/\mathrm{ARL}_0)\mathbf{n} \tag{21}$$

We refer to expected relative frequencies instead of to steady-state probabilities because the chain is not ergodic. Lucas and Saccucci [16] use the term "cyclical steady-state probabilities", and the elements of $\mathbf{r}$ may be considered as such, taking into account that the monitoring is reinitiated after every alarm.

The expected relative frequency, p_0, of visits to states corresponding to $WL < Z_t \le UCL$ during the in-control phase is therefore

$$p_0 = \sum_{k=A+1}^{M} r_k \tag{22}$$

and the average sampling interval during the in-control phase, $\overline{h}$, is

$$\overline{h} = h_S p_0 + h_\mathrm{L}(1 - p_0) \tag{23}$$

Hence, the specification by the user of a value for $\overline{h}$ determines the value of h_L as a function of h_S:

$$h_\mathrm{L} = \left(\overline{h} - h_\mathrm{S} p_0\right)/(1 - p_0) \tag{24}$$

Now let us define a vector $\mathbf{h}$ of dimension M, whose first A elements are equal to h_L and the remaining B elements are equal to h_S. The ATS_0 can be obtained as:

$$\mathrm{ATS}_0 = \mathbf{n'h} \tag{25}$$

(alternatively, it is also true that $\mathrm{ATS}_0 = \mathrm{ARL}_0\overline{h}$. The demonstration of the equivalence of these two expressions is omitted for reasons of space.)

The steady-state average time-to-signal, ATS_1, is the expected time between the last sample before the upward shift in the nonconformities rate and the true alarm and is given by

$$\mathrm{ATS}_1 = \mathbf{w'N_1h} \tag{26}$$

where $\mathbf{w}$ is the vector of initial state probabilities for the out-of-control phase, given by

$$\mathbf{w} = \frac{\mathrm{diag}(r_1, r_2, \ldots, r_M)\mathbf{h}}{\mathbf{r'h}} \tag{27}$$

This equation can be explained as follows: The probability that the chain is in a given state when the shift occurs is equal to the expected fraction of time the chain spends in that state during the in-control phase, and this expected fraction of time is in its turn proportional to the product of the length of the sampling interval associated to that state by the expected relative frequency of visits to it during the in-control phase.

The expected time between the shift in c and the alarm, called AATS, is equal to the ATS_1 minus the expected value of the time interval T between the last sample of the in-control phase and the time of occurrence of the shift, that is,

$$\mathrm{AATS} = \mathrm{ATS}_1 - \mathrm{E}(T) \tag{28}$$

Assuming, like Reynolds et al. [26], that the conditional probability density of the instant of the shift between two given consecutive samples is very well approximated by a uniform distribution between these two sampling times, the expected value of T becomes

$$E(T) = \mathbf{w'h}/2 \tag{29}$$

where $\mathbf{w}'\mathbf{h}$ is the expected length of the sampling interval between the last sample of the in-control phase and the first sample after the shift (incidentally, it is easy to verify that $\mathbf{w'h} = p_0 h_\mathrm{S}^2 + (1 - p_0)h_\mathrm{L}^2$).

[13] report that this approximation for $E(T)$ is very precise if h_S and h_L are smaller than 10% of the duration of the in-control phase. From Eqs. 26, 28, and 29,

$$\mathrm{AATS} = \mathbf{w'N_1h} - \mathbf{w}'\mathbf{h}/2 \tag{30}$$

References

1. Annadi HP, Keats JB, Runger GC, Montgomery DC (1995) An adaptive sample size CUSUM control chart. Int J Prod Res 33:1605–1616
2. Arnold JC, Reynolds MR Jr (1994) CUSUM charts with variable sample size and variable interval size. Proceedings, Section on Quality and Productivity, ASA, pp 132–137
3. Borror CM, Champ CW, Rigdon SE (1998) Poisson EWMA control charts. J Qual Technol 30(4):352–361
4. Brook D, Evans DA (1972) An approach to the probability distribution of CUSUM run length. Biometrika 59(3):539–549
5. Capizzi G, Masarotto G (2003) An adaptive exponentially weighted moving average control chart. Technometrics 45 (3):199–207
6. Costa AFB (1994) $\overline{X}$ charts with variable sample size. J Qual Technol 26(3):155–163
7. Costa AFB (1997) $\overline{X}$ charts with variable sample size and sampling intervals. J Qual Technol 29(2):197–204
8. Costa AFB (1998) Joint $\overline{X}$ and R charts with variable parameters. IIE Trans 30:505–514
9. Costa AFB (1998) VSSI Xbar charts with sampling at fixed times. Commun Stat Theory Methods 27(11):2853–2869
10. Costa AFB (1999) Joint $\overline{X}$ and R charts with variable sample size and sampling intervals. J Qual Technol 31:387–397
11. Costa AFB (1999) $\overline{X}$ charts with variable parameters. J Qual Technol 31(4):408–416
12. Epprecht EK, Costa AFB (2001) Adaptive sample size control charts for attributes. Qual Eng 13(3):465–473
13. Epprecht EK, Costa AFB, Mendes FCT (2003) Adaptive control charts for attributes. IIE Trans 35(6):567–582
14. Gan FF (1990) Monitoring observations generated from a binomial distribution using modified exponentially weighted moving average control chart. J Stat Comput Simul 37(1):45–60
15. Gan FF (1990) Monitoring Poisson observations using modified exponentially weighted moving average control charts. Commun Stat Simul Comput 19(1):103–124
16. Lucas JM, Saccucci MS (1990) Exponentially weighted moving average control schemes: properties and enhancements. Technometrics 32(1):1–12
17. Luo H, Wu Z (2002) Optimal *np* control charts with variable sample sizes or variable sampling intervals. Econ Qual Control 17(1):39–61
18. Montgomery DC (2001) Introduction to statistical quality control, 4th edn. Wiley, New York
19. Prabhu SS, Runger GC, Keats JB (1993) $\overline{X}$ chart with adaptive sample sizes. Int J Prod Res 31(12):2895–2909
20. Prabhu SS, Montgomery DC, Runger GC (1994) A combined adaptative sample size and sampling interval $\bar{x}$ control scheme. J Qual Technol 26(3):164–176
21. Reynolds MR Jr (1989) Optimal variable sampling interval control charts. Seq Anal 8:361–379
22. Reynolds MR Jr (1995) Evaluating properties of variable sampling interval control charts. Seq Anal 14:59–97
23. Reynolds MR Jr (1996) Shewhart and EWMA variable sampling interval control charts with sampling at fixed times. J Qual Technol 28:199–212
24. Reynolds MR Jr, Arnold JC (1989) Optimal one-sided Shewhart control charts with variable sampling intervals. Seq Anal 8:51–77
25. Reynolds MR Jr, Arnold JC (2001) EWMA control charts with variable sample sizes and variable sampling intervals. IIE Trans 33:511–530
26. Reynolds MR, Amin RW, Arnold JC, Nachlas JA (1988) $\overline{X}$ charts with variable sampling intervals. Technometrics 30(2):181–192
27. Reynolds MR, Amin RW, Arnold JC (1990) CUSUM charts with variable sampling intervals. Technometrics 32:371–384
28. Runger GC, Pignatiello JJ Jr (1991) Adaptive sampling for process control. J Qual Technol 23:135–155
29. Runger GC, Montgomery DC (1993) Adaptive sampling enhancements for Shewhart control charts. IIE Trans 25:41–51
30. Saccucci MS, Amin RW, Lucas JM (1992) Exponentially weighted moving average control schemes with variable sampling intervals. Commun Stat Simul Comput 21:627–657
31. Sawalapurkar U, Reynolds MR Jr, Arnold JC (1990) Variable sampling size $\overline{X}$ control charts. Presented at the Winter Conference of the American Statistical Association, Orlando FL
32. Tagaras G (1998) A survey of recent developments in the design of adaptive control charts. J Qual Technol 30(3):212–231
33. Trevanich A, Bourke P (1993) EWMA control charts using attributes data. The Statistician 42(3):215
34. Vaughan TS (1993) Variable sampling interval *np* process control chart. Commun Stat Theory Methods 22(1):147–167
35. Zimmer LS, Montgomery DC, Runger GC (1998) Three-state sample size $\overline{X}$ chart. Int J Prod Res 36:733–743